Journal of Radioanalytical and Nuclear Chemistry (2021) 330:529–538
https://doi.org/10.1007/s10967-021-07866-x

Phase analysis of iron oxides forming the red pigment layer of the ancient earthenwares excavated from the southern Korean Peninsula

Min Hye Lee[1] · Min Su Han[1] · Young Rang Uhm[2] · Chul Sung Kim[3]

Received: 20 February 2021 / Accepted: 22 June 2021 / Published online: 25 July 2021
© Akadémiai Kiadó, Budapest, Hungary 2021

Abstract
It is assumed that clay soil with high Fe contents as its main ingredient was used in the red pigment layers on the surfaces of the Neolithic Age Red Painted pottery and the Red Burnished pottery in the Bronze Age that were excavated from the southern areas of the Korean peninsula. A variety of phases of iron oxides that form pigment layers were identified through X-ray diffraction analysis, Raman spectroscopy and Mössbauer spectroscopy in this study. In particular, although previous studies focused only on hematite as a pigment mineral, the Mössbauer spectra of pigment layers in this study showed a higher spectrum area ratio of sextet by ferrihydrite than that by hematite, implying that ferrihydrite in reddish-brown might have played a significant role in developing its color. In addition, as it can be seen in each specimen showing a different area ratio by site in the Mössbauer spectrum, compositions of Fe-containing minerals were different. It is assumed to have been caused by different ionic forms of iron in the soil materials and unstable firing atmosphere during Pit firing.

Keywords Mössbauer spectroscopy · X-Ray Diffraction analysis · Raman spectroscopy · Red Burnshied Pottery · Fe phase

Introduction

Potteries are used as indicators of ages as their shapes and manufacturing techniques were developed following respective eras. In particular, red-painted potteries manufactured during the prehistoric age are found worldwide, most of which were designed for rituals and buried.

The use of earthenwares in Korea was at least from 8,000 B.C., in accordance with the relics in Gosan-ri site, Jeju. From the Neolithic Age, the Red Painted pottery, which is called *Juchil* (in Korean, red-painted) pottery, was made with red pigment applied to the outer surface, and a burnishing technique for polishing the surface of earthenware was introduced [1]. It is known that the surface is semi-dry during burnishing process and flattened using various tools such as pebbles and leaves to enhance the coloration and polish effect [1, 2]. The burnishing technique reduces absorption by fine-tuning the surface, and was used as a common method of making even surfaces of prehistoric earthenware. The neolithic red painted pottery and the red burnished pottery were excavated mainly in the southern part of the Korean Peninsula.

A prior study of the Neolithic Age Red Painted pottery and the Red Burnished pottery on the Korean Peninsula has confirmed that iron (Fe) is the main element of pigmentation [3, 4]. In addition, some studies conducted X-ray diffraction analysis of samples of red painted pottery and red burnished pottery, and hematite (α-Fe_2O_3) was identified to present red iron as the main source of coloration of the red pigmentation layer [4]. Estimates of materials in the pigmentation layer were based on microscopic observance and SEM–EDS analysis, and minerals were directly analyzed using XRD analysis in few reaserches, but only a weak peak of hematite was identified, and Phase analysis of iron oxides forming the red pigment layer was insufficient.

✉ Min Su Han
dormer@korea.kr

[1] Department of Heritage Conservation and Restoration, Graduate School of Cultural Heritage, Korea National University of Cultural Heritage, Buyeo 33115, Republic of Korea

[2] HANARO Utilization Division, Korea Atomic Energy Research Institute (KAERI), Daejeon 34057, Republic of Korea

[3] Department of Nano-Electro Physics, Kookmin University, Seoul 02707, Republic of Korea

Mössbauer spectroscopy is an ionic phase analysis method using gamma-ray resonance, and the study of pottery using Mössbauer spectroscopy confirms that the phase analysis of the mineral that consists the pottery is possible [5–10]. The studies have been conducted on the phase transition of minerals according to the firing atmosphere. Since the phase of the Fe-containing minerals in the red painted pottery and the red burnished pottery depends on the raw materials and firing conditions used to produce the red color, it can provide crucial information on the production techniques.

Therefore, room temperature Mössbauer spectroscopy using Fe-57 was applied on a trial basis to analyze the crystalline phase of the Fe-containing minerals in the pigment layers of ancient earthenware excavated from the Southern Korean Peninsula. Prior to the Mössbauer spectroscopy analysis, Fe content was analyzed using SEM–EDS and elemental distribution on the cross-section of the pigment layer was verified through elemental map. Crystal structure analysis using XRD and Raman spectroscopy confirmed the existence of iron oxides, the most influential composition of the pigment layer, and the results of different analysis methods were cross-validated.

Experimental

Sample preparation

For the analysis of excavated specimens, the samples with well-preserved surfaces and no traces of conservation treatment were selected from the collection of the National Jinju Museum. Additional samples were provided with good surface preservation with the help of other institutions and related researchers. The three Neolithic Age Painted pottery and the five Red Burnished pottery were analyzed Table 1, Fig. 1 and Fig. 2. The Red Burnished pottery JJ-1 and other Bronze Age pottery

Fig. 1 Location of the archaeological sites for study

samples excavated from Sancheong were provided by Jinju National Museum. Kyungnam University Museum provided the Red Burnished pottery JJ-7, and the Neolithic pottery samples from Geoje and Tongyeong were provided by Gimhae national Museum. The Neolithic pottery sample UJ-1 excavated from Jukbyeon-ri site was provided by Samhan Institute of Cultural Properties.

Color

The surface colors of potteries are affected by the chemical composition of raw materials and firing conditions. Therefore, the firing intensity and conditions can be inferred by the color information, and chromaticity was measured to understand the correlation between iron oxide phases and

Table 1 List of the pottery samples analyzed in this study

Sample	Age	Type	Site
JJ-4	Bronze Age	The Red Burnished Pottery	Daepyeong-ri site, Jinju
JJ-7			Daepyeong-ri site, Jinju
SCG-1			Maechon-ri site, Sancheong
SCG-2			Maechon-ri site, Sancheong
SCG-5			Maechon-ri site, Sancheong
UJ-1	Neolithic Age	The Red Painted Pottery	Jukbyeon-ri site, Uljin
TY-3			Yondaedo Shell Midden, Tongyeong
GJ-1			Daepo Shell Midden, Geoje

colors. The external chromaticity of all specimens was measured by a portable Chroma meter (CR-400, Minolta, Japan) after the specimens were dried entirely To reduce measurement error, average values of 3 measurements were used. The measurement results were displayed in L*, a*, and b* chromatic systems.

Elemental composition: SEM–EDS

For the composition analysis of excavated potteries, an energy dispersive X-ray spectrometer attached to a scanning microscope was used. The surfaces of the potteries made as mounting specimens were magnified to 300×, and elemental mapping was performed to check the Fe content of the surface pigment layer.

Constituent minerals: XRD and raman spectroscopy

To identify compositional minerals, crystal structures were analyzed with an X-ray diffraction spectroscope (Miniflex600, Rigaku, Japan). After contaminated surfaces of specimens were washed with distilled water, red pigment layers were extracted from the surfaces using a scalpel to prevent mixing with clay, powdered, and completely dried at 100 ± 5℃ for over 24 h. The analysis condition was set to 40 kV, 15 mA, 5°–80°, scan step of 0.02°, and scan speed of 1°/min.

The pottery surfaces were further analyzed using a micro-Raman spectrometer (LamRAM Aramis, Horiba, Japan) with a laser of 785 nm, 10× objectives. The data of the Raman spectrum was compared to the hematite (α-Fe_2O_3), magnetite (Fe_3O_4), and goethite (α-FeO(OH)) spectral data analyzed using 785 nm laser in the RRUFF Project website. However, the analysis was expected to be challenged as iron oxides are easily denatured by laser, and it occurs even faster when the crystallinity is not high in a natural state [11]. Thus, specimens with the well preserved surface pigment layer were selected for the analysis, observed for any changes in spectrums before and after the analysis, and then verified any discoloration through microscopic images.339A

Phase of Fe ion: mössbauer spectroscopy

Mössbauer spectroscopy was conducted by the Department of Physics of Kookmin University, to verify crystalline characteristics of iron oxides in red layers. The measurement was carried out at room temperature through an electrodynamic constant-acceleration Mössbauer spectrometer using a single light source of Co-57 at 50 mCi dispersed on Rh metal of FAST (MR-31, driving unit). The specimen used as an absorber was applied as a thin layer between Al foils of 1 inch diameter, and both sides were blocked and fixed with 0.125 inches thick Be plates. The fixed specimen was secured on a specimen holder made of Cu to maintain consistent temperature across the specimen during the measurement.

Results and discussion

Color and elemental composition of the pigment layer

The iron oxide content of the pigment layers measured by SEM–EDS analysis was compared to the intensity of the red color of the specimen surfaces to illustrate a regression line passing through the center point and 95% confidence interval Fig. 3. The degree of scattering is determined by various phases of iron oxide generated by differences in the firing conditions of the pigment layers. It seems that the pigmentation was affected by the conservation status and mineral composition of the pigment layers. However, as thinner and poorly preserved pigment layers mean less shield from the clay material, the chromaticity value may reflect the color of the clay material. As an example of color change due to the change in Fe phase, the previous research verified that while only a* value increases when the phase is changed from ferrihydrite to goethtite, both a* and b* values increase simultaneously when it is changed to hematite [12].

Constituent minerals

Figure 4. The peaks of hematite of the (140) planes appeared at 33° and near 35.7° where its (110) planes. As for the γ phase, the peak of maghemite near 35.6° of the (311) planes and near 30.2° of the (220) planes, overlaps with the peak of

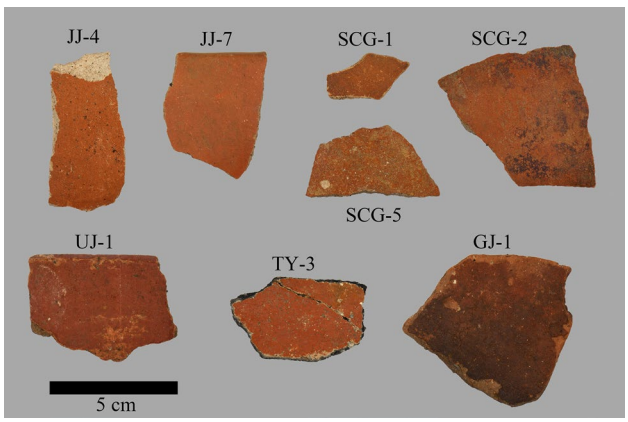

Fig. 2 the red painted pottery sherds analyzed in this study

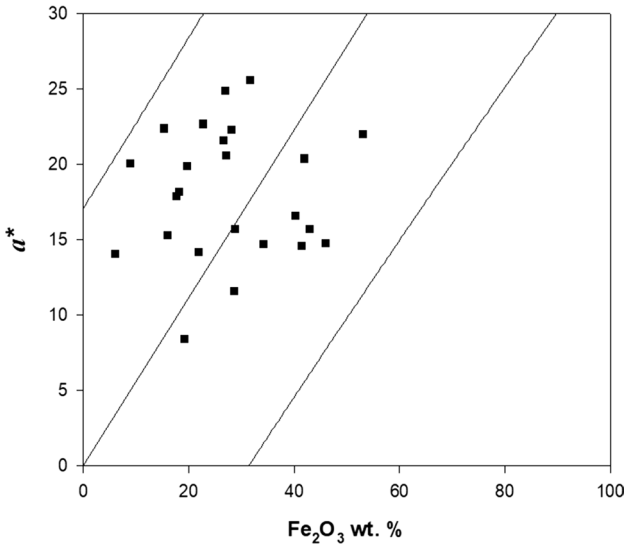

Fig. 3 Iron oxides content analyzed by SEM–EDS vs. a* value of the pigment layer, regression line and the line at the endpoints of the 95% confidence intervals

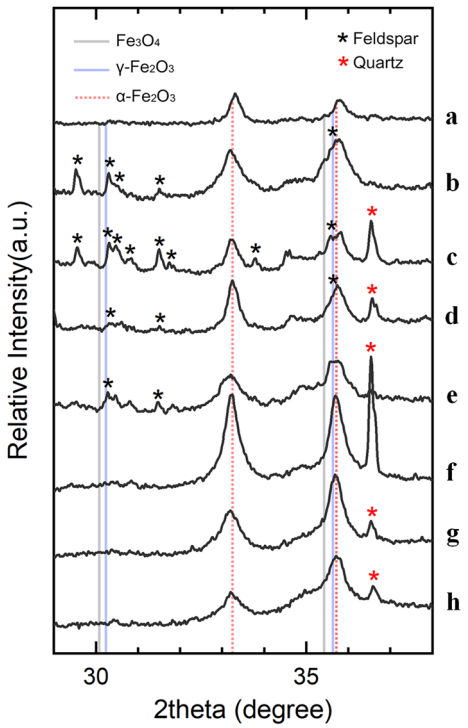

Fig. 4 XRD spectra of the pigment layers of pottery sherds for **a** JJ-4, **b** JJ-7, **c** SCG-1, **d** SCG-2, **e** SCG-5 **f** UJ-1, **g** TY-3 and **h** GJ-1

feldspar group, did not appear. Also, the peak of magnetite did not appear near 30.1° on the (220) planes.

On the other hand, ferrihydrite shows a two-line or a five-line pattern in the X-ray diffraction analysis, but as it has X-ray amorphous characteristics, it is difficult to identify when analyzed along with crystalline material. Although the main peak of lepidocrocite is relatively easy to identify in XRD, it was not identified in the analysis result.

Raman spectra of the pigment layers showed that hematite had a 403–411 cm^{-1} peak due to Fe–O bending and a 594–600 cm^{-1} peak due to Fe–O stretching along with a broad peak near 1310 cm^{-1} Fig. 5. In addition, it was confirmed that magnetite had a 671–674 cm^{-1} peak due to asymmetric stretching and a 520–240 cm^{-1} peak due to Fe–O asymmetric bending. The Raman band of the pigment layers did not show any goethite, which is relatively common in soil, like the XRD diffraction pattern. Although it can be a relative difference in contents in the pigment layer, it is assumed that the phase of most goethite of the raw material was changed to hematite as it went through the firing process.

Phase of Fe ion

In the Mössbauer spectra of the pigment layers, a sextet by α-Fe_2O_3, 2 sextets by Fe_3O_4, and a doublet by ferrihydrite or γ-FeO(OH) were overlapped for all the specimens Fig. 6. Table 2 shows the hyperfine field (Hhf), the quadrupole

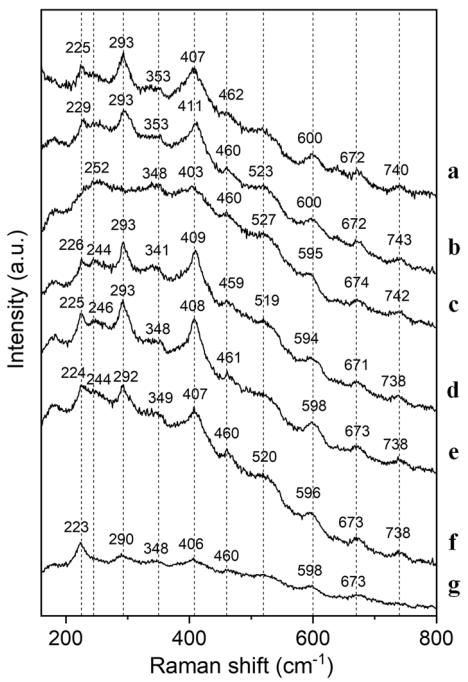

Fig. 5 Raman spectra of the pigment layers of pottery sherds for **a** JJ-4, **b** JJ-7, **c** SCG-1, **d** SCG-2, **e** UJ-1, **f** TY-3 and g GJ-1

Table 2 Mössbauer parameter of the red pigments collected from pottery sherds

Sample	Site	Fe phase	Hhf (kOe)	ΔE_Q (mm/s)	δ (mm/s)	Area (%)
JJ-4	α-Fe_2O_3	Fe(III)	510.18	−0.10	0.25	23.57
	Fe_3O_4 A-site	$Fe(III)_{Td}$	506.11	−0.09	0.24	9.13
	Fe_3O_4 B-site	$Fe(II)Fe(III)_{oh}$	463.53	0.00	0.46	13.76
	Ferrihydrite	Fe(III)	–	0.80	0.17	53.43
JJ-7	α-Fe_2O_3	Fe(III)	501.75	−0.08	0.23	34.77
	Fe_3O_4 A-site	$Fe(III)_{Td}$	497.34	−0.09	0.31	10.51
	Fe_3O_4 B-site	$Fe(II)Fe(III)_{oh}$	458.19	−0.14	0.44	16.75
	Ferrihydrite	Fe(III)	–	0.82	0.22	38.25
SCG-1	α-Fe_2O_3	Fe(III)	510.70	−0.12	0.27	21.01
	Fe_3O_4 A-site	$Fe(III)_{Td}$	502.25	−0.04	0.32	10.50
	Fe_3O_4 B-site	$Fe(II)Fe(III)_{oh}$	468.65	−0.11	0.45	15.88
	Ferrihydrite	Fe(III)	–	0.73	0.18	52.61
SCG-2	α-Fe_2O_3	Fe(III)	511.60	−0.10	0.22	21.76
	Fe_3O_4 A-site	$Fe(III)_{Td}$	502.96	−0.08	0.32	7.44
	Fe_3O_4 B-site	$Fe(II)Fe(III)_{oh}$	469.61	−0.15	0.42	10.96
	Ferrihydrite	Fe(III)	–	0.75	0.21	59.84
SCG-5	α-Fe_2O_3	Fe(III)	504.00	−0.07	0.20	34.31
	Fe_3O_4 A-site	$Fe(III)_{Td}$	500.25	−0.05	0.32	12.03
	Fe_3O_4 B-site	$Fe(II)Fe(III)_{oh}$	466.65	−0.11	0.44	19.08
	Ferrihydrite	Fe(III)	–	0.69	0.23	34.58
UJ-1	α-Fe_2O_3	Fe(III)	505.00	−0.09	0.22	22.62
	Fe_3O_4 A-site	$Fe(III)_{Td}$	502.76	−0.03	0.32	9.21
	Fe_3O_4 B-site	$Fe(II)Fe(III)_{oh}$	470.71	−0.02	0.44	15.79
	Ferrihydrite	Fe(III)	–	0.72	0.24	52.39
TY-3	α-Fe_2O_3	Fe(III)	507.28	−0.08	0.25	36.98
	Fe_3O_4 A-site	$Fe(III)_{Td}$	505.96	−0.21	0.25	12.29
	Fe_3O_4 B-site	$Fe(II)Fe(III)_{oh}$	472.26	−0.06	0.45	17.18
	Ferrihydrite	Fe(III)	–	0.72	0.22	33.55
GJ-1	α-Fe_2O_3	Fe(III)	505.05	−0.06	0.27	32.59
	Fe_3O_4 A-site	$Fe(III)_{Td}$	503.25	−0.04	0.25	8.15
	Fe_3O_4 B-site	$Fe(II)Fe(III)_{oh}$	465.65	−0.11	0.52	12.58
	Ferrihydrite	Fe(III)	–	0.72	0.26	46.69

splitting (ΔE_Q), theisomer shift (δ), and the area ratios of spectrum by site.

In the Mössbauer spectrum measured at room temperature, it is challenging to distinguish hematite (α-Fe_2O_3) on α-phase from maghemite (γ-Fe_2O_3) on γ-phase. However, considering that the results of X-ray diffraction analysis and Raman spectroscopy showed a stronger peak of hematite and that the particle size effect might have reduced the values in the hyperfine field, the sextets of 501.75–511.66kOe identified in each specimen are likely to have been generated by α-Fe_2O_3. It has been reported that α-Fe_2O_3 measured at room temperature has a sextet with a wide range of values around the hyperfine field of 518kOe, the isomer shift of 0.37 mm/s, the quadrupole splitting of − 0.2 mm/s [12].

The X-ray diffraction analysis did not show any peak of ferrihydrite or lepidocrocite, while the Mössbauer analysis showed a very high spectrum area ratio of 33.55–59.84%. At room temperature, lepidocrocite is identified as a doublet having values of the isomer shift of 0.37 mm/s and the quadrupole splitting of 0.53 mm/s, and has a similar resonance absorption line to ferrihydrite. However, it is characterized by a lower quadruple splitting and narrower line width [13, 14]. The sample measured in this study resulted in the quadrupole splitting value of 0.72–0.8 mm/s, which is somewhat

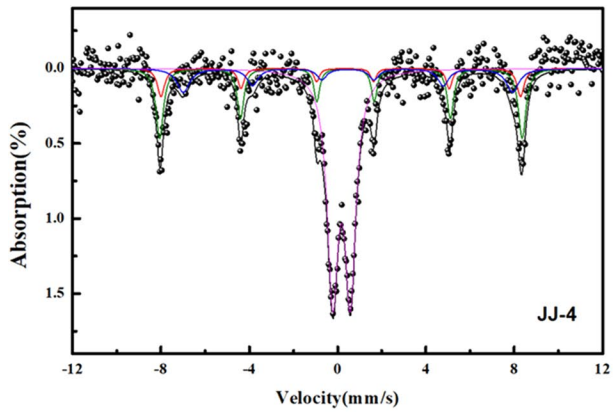
Absorption(%)
Velocity(mm/s)
JJ-4

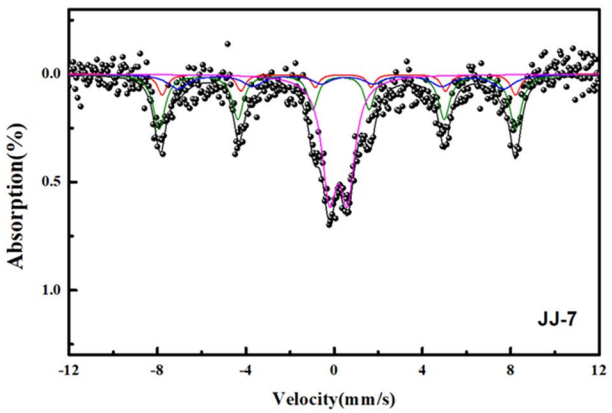
Absorption(%)
Velocity(mm/s)
JJ-7

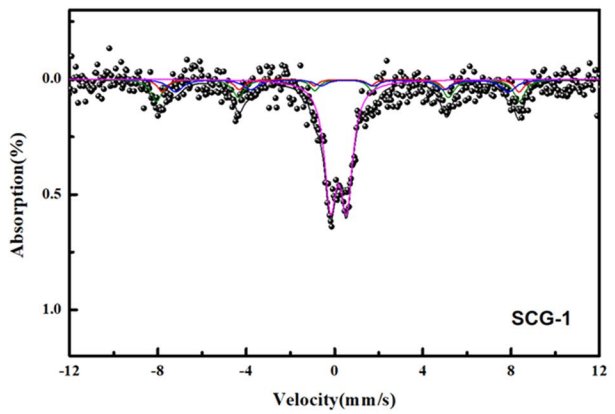
Absorption(%)
Velocity(mm/s)
SCG-1

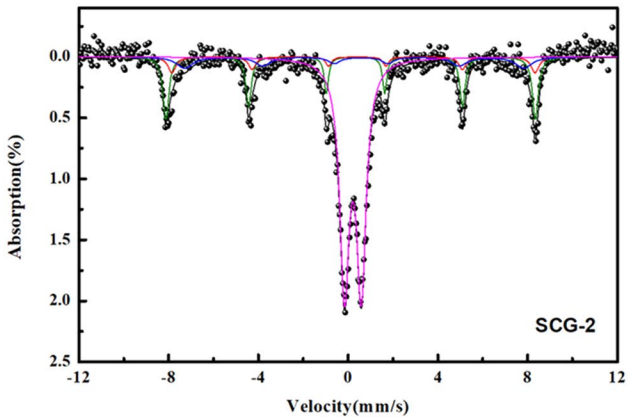
Absorption(%)
Velocity(mm/s)
SCG-2

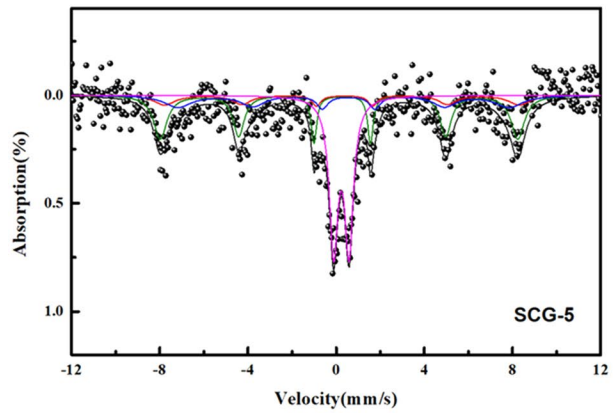
Absorption(%)
Velocity(mm/s)
SCG-5

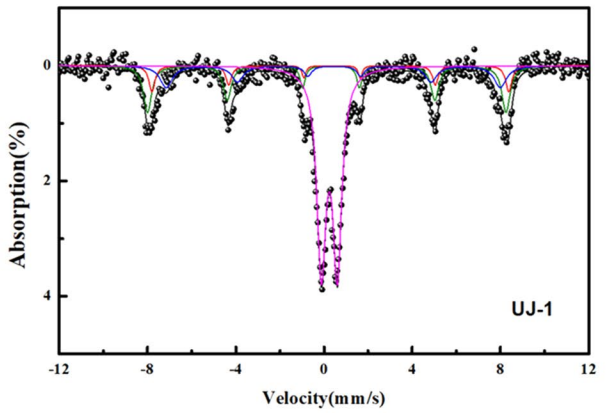
Absorption(%)
Velocity(mm/s)
UJ-1

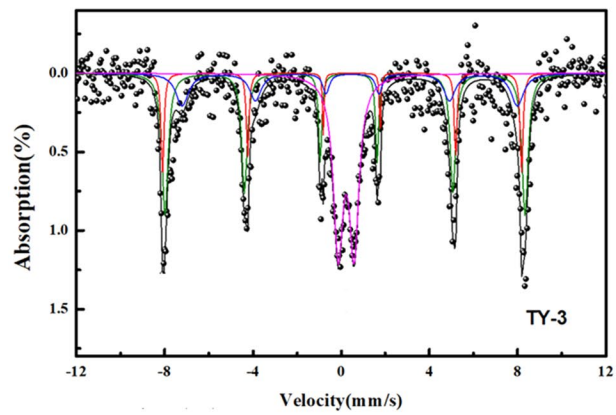
Absorption(%)
Velocity(mm/s)
TY-3

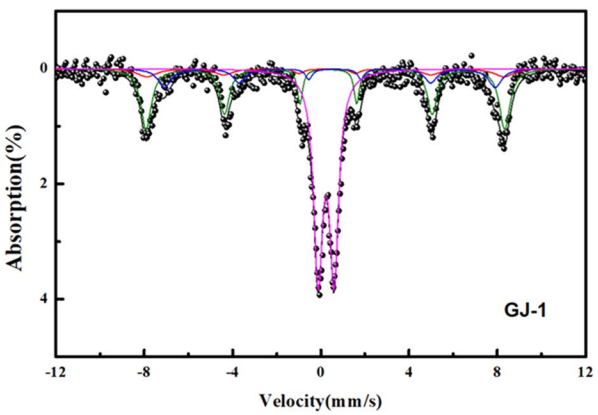
Absorption(%)
Velocity(mm/s)
GJ-1

◂**Fig. 6** Mössbauer spectra of the red pigment layers. The black dots represent the raw data collected as Mossbauer spectra. The green lines refer to α-Fe_2O_3, and red and blue lines to each A site and B site of Fe_3O_4, respectively. Pink lines refer to ferrihydrite

higher than that of lepidocrocite, and a wider line as well. Therefore, it was identified as ferrihydrite.

Lepidocrocite forms maghemite in a semi-stable state at approximately 473–553 K during firing at oxidizing atmosphere [14], and it goes through a phase transition to hematite at about 873 K as the temperature rises [15].

$$\gamma - \mathrm{FeO(OH)} \rightarrow {}^{1}\!/_{2}\gamma - \mathrm{Fe_2O_3} + {}^{1}\!/_{2}\mathrm{H_2O}$$

$$\gamma - \mathrm{Fe_2O_3} \rightarrow \alpha - \mathrm{Fe_2O_3}$$

Soil contains abundant α-phase goethite [α-FeO(OH)], which forms hematite when fired at 530—600 K [7, 14]. The Red Burnished pottery is assumed to have been fired at 873 K or higher, so most of the iron hydroxide in soil was expected to have gone through a phase transition to hematite immediately after firing.

As for an inverse spinel structure of magnetite (Fe_3O_4), in a cell unit of the face-centered cubic, Fe^{3+} ions occupy 8 A sites with tetrahedron symmetry, and 8 Fe^{2+} ions and 8 Fe^{3+} ions occupy 16 B sites with octahedron symmetry. The Mössbauer spectrum of Fe_3O_4 at room temperature shows two sextets overlapped with each other because of the presence of the two different grid sites []. Reduction firing generates magnetite via reaction to carbon monoxide, while oxidized firing generates hematite.

$$3\mathrm{Fe_2O_3} + \mathrm{CO} \rightarrow 2\mathrm{Fe_3O_4} + \mathrm{CO_2}$$

$$2\mathrm{Fe_3O_4} + {}^{1}\!/_{2}\mathrm{O_2} \rightarrow 3\alpha - \mathrm{Fe_2O_3}$$

Comparison of spectrum area ratios for each site in the Mössbauer spectrum showed a complete inverse proportional relationship where the area ratio of ferrihydrite decreases as the α-Fe_2O_3 phase increases, and ferrihydrite increases as the area of the α-Fe_2O_3 phase decreases Fig. 7. Area ratios of α-Fe_2O_3 and Fe_3O_4 tend to increase or decrease concurrently, but they do not show increase/decrease curves that are perfectly consistent. Therefore, an increase/decrease in the area ratios of α-Fe_2O_3 and Fe_3O_4 is inversely proportional to ferrihydrite. Fe_3O_4 detected in specimens after firing implies a possible presence of different iron oxyhydroxides from the soil. If some lepidocrocite existed in the soil, maghemite, which is an intermediate product of lepidocrocite and hematite, was potentially existed in the specimens as well, considering the firing reaction. In this case, the spectrum might have been overlapped with hematite. Since iron oxides may exist in various phases, an additional Mössbauer measurement needs to be conducted at a lower temperature (4.2 K) for accurate assessment in the further study.

In order to understand the effect of iron content in pigment layers forming hematite during oxidized firing and the oxidation–reduction of Fe ions on the chromaticity, the relationship between the spectrum area of α-Fe_2O_3 and the chromaticity value is illustrated on a 2-dimensional plane and the stoichiometry Fe(II)/Fe(III) for each specimen was calculated Table 3. The following formula was used with relative area ratios of A site and B site sextets to obtain the stoichiometry ratio of Fe ions within Fe_3O_4 [16].

$$\left[\mathrm{Fe(II)/Fe(III)}\right]_{\mathrm{Fe3O4}} = \left(0.5 \times \mathrm{Fe_{Oh}}\right) / \left(0.5 \times \mathrm{Fe_{Oh}} + \mathrm{Fe_{Td}}\right)$$

The comparison between the α-Fe_2O_3 area ratio and the chromaticity did not show any relations between the increase in α-Fe_2O_3 area ratio and the increase/decrease in certain chromaticity value Fig. 8. The area ratio of ferrihydrite phase increase/decrease shows an inverse proportion to α-Fe_2O_3 phase and Fe_3O_4 phase, implying that the black Fe_3O_4 affected the increase/decrease in the chromaticity value. However, if pottery contains red γ-FeO(OH that can only be identified via measurement at a lower temperature (4.2 K), they might collectively influence on of the pigment layers. The higher the Fe(II)/Fe(III) value, the more

Table 3 Stoichiometry ratio of Fe ion and L*a*b* values of pigment layers

Type	Sample	Area (%)			Color		
		Fe(II)	Fe(III)	Fe(II)/Fe(III)	L*	a*	b*
BA	JJ-4	6.88	93.01	0.07	50.3	20.6	26.7
	JJ-7	8.38	91.91	0.09	48.0	19.9	24.3
	SCG-1	7.94	92.06	0.09	48.0	20.1	28.3
	SCG-2	5.48	94.52	0.06	46.6	18.2	22.1
	SCG-5	9.54	90.46	0.11	49.3	14.2	24.4
NA	UJ-1	7.90	92.12	0.09	44.6	25.6	29.3
	TY-3	8.59	91.41	0.09	41.0	22.3	21.2
	GJ-1	6.29	93.72	0.07	35.8	15.7	18.3

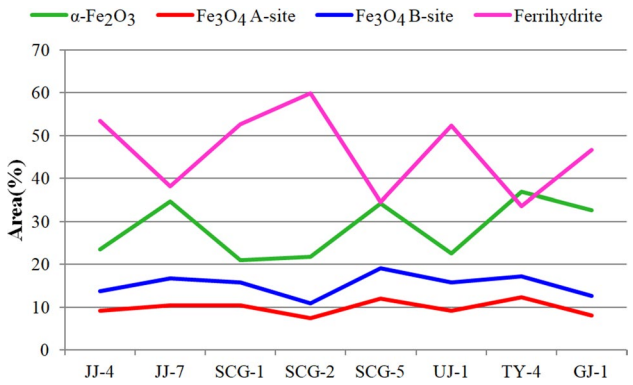

Fig. 7 Area ratio of the Mössbauer spectra collected from pigment layers

intense the reduction atmosphere is likley to be established. Accordingly, The analyzed potteries in this study showed the Fe(II)/Fe(II) values between 0.06 and 0.11, which is significantly lower than those of celadon glaze (2.5 – 7) fired at a reducing atmosphere [17]. Although the area ratio of Fe(II)/Fe(III) and chromaticity did not show any distinct relationship between the two, it might have been affected by the texture of the surfaces or particle sizes.

Conclusions

Previous studies argued that hematite α-Fe_2O_3, which was identified in X-ray diffraction analysis, led the pigmentation of Neolithic and Bronze Age potteries excavated in the Korean peninsula. However, Raman spectroscopy and Mössbauer spectroscopy used in this study identified various phases of iron oxides that previous studies failed to detect or identify due to very weak peaks. In particular, the Mössbauer spectrum showed that the Fe_3O_4 phase affected the pigmentation, and the spectrum area ratio of the sextets generated by the phase assumed as ferrihydrite (some might be lepidocrocite) was significantly higher than that of hematite, indicating that ferrihydrite might have contributed to the pigmentation. In addition, each specimen had different area ratio of each site in the Mössbauer spectrum, demonstrating different content of minerals including iron. This can be attributed to the Fe phases in soil and the unstable firing atmosphere during open pit firing. There was difficulty in obtaining specimens with different colors and iron oxide contents due to the characteristics of the excavated artifact. However, this study demonstrated strengths of the Mössbauer method in analyzing ferruginous mineral pigments, which have been used since the ancient times. The specimen produced through its reproduction experiment will allow scientifical interpretation of the relationships between generated iron oxides, chromaticity and firing atmosphere.

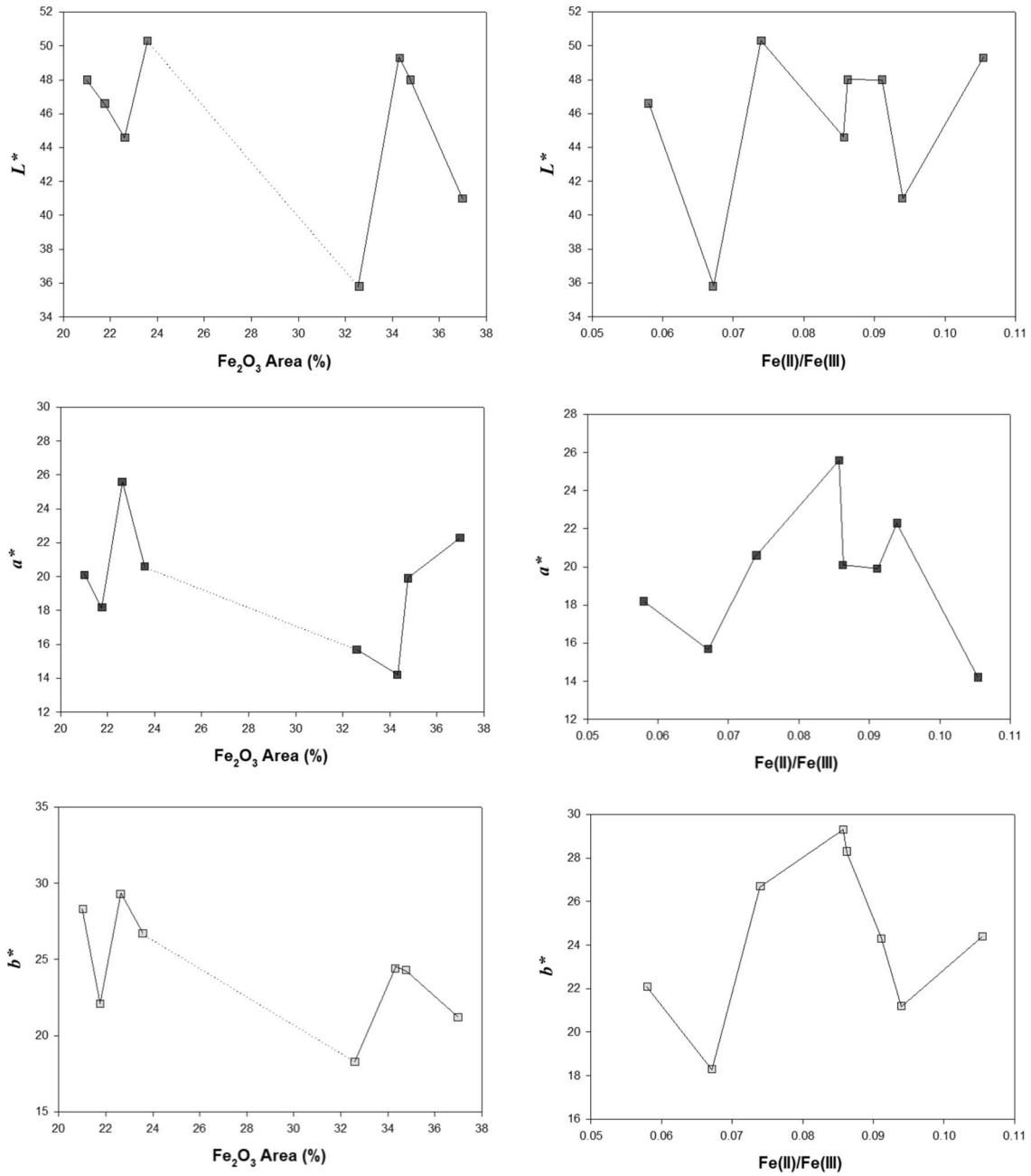

Fig. 8 Variation in L*a*b* values with area ratio of α -Fe_2O_3 and Fe(II)/Fe(III)

Acknowledgements The samples used in this study were provided by the Jinju National Museum in Korea, and we are grateful for this.

References

1. Song YJ (2016) A study on the burnished pottery of Bronze Age Korea Peninsula. Dept. of History, Doctoral thesis, Graduate School of Gyeongsang National University, Jinju **(in Korean with English abstract)**
2. Nam SW (2013) As production technology, the meaning of the Black burnished pottery in Baekje Dynasty. J Korean Archaeol Soc 89:94–137 **(in Korean with English abstract)**
3. Cho HJ, Yang SR (1988) Pottery analysis of Songguk-ri site, Sinam-ri I. Natl Mus Hist Sites Res Rep 20:118–119 **(in Korean)**
4. Han JU (2010) Study on the material characteristics of the red burnished potteries from gangwon region, Korea: focusing on Osan-ri in Yangyang, Daedae-ri in Goseong, Jucheon-ri on Yeongwol. Master's thesis, Dept. of Cultural Heritage Conservation Science, Graduate School of Kong Ju National University, Gonju **(in Korean with English abstract)**

5. Bouchez R, Coey J, Coussement R, Schmidt K, van Rossum M, Aprahamian J, Deshayes J (1974) Mössbauer study of firing conditions used in the manufacture of the grey and red ware of Tureng-Tepe. J Phys Colloq 35(C6):541–546. https://doi.org/10.1051/jphyscol:19746115
6. Kostikas A, Simopoulos A (1974) Mössbauer studies of ancient pottery. J Phys Colloq 35(C1):107–115. https://doi.org/10.1051/jphyscol:1974133
7. Maggetti M (1982) Phase Analysis and Its Significance for Technology and Origin. Archaeological Ceramics, Smithsonian Institution Press, Washington, D.C.
8. Venkatachalapathy R, Gournis D, Manoharan C, Dhanapandian S, Deenadayalan K (2003) Application of FTIR and Mössbauer spectroscopy in analysis of some South Indian archaeological potteries. Indian J Pure Appl Phys 41:833–838
9. Amzal M, Bouhas A, Benchaba H (1996) Mössbauer studies of Algerian ancient pottery. J Radioanal Nucl Chem 213:193–198. https://doi.org/10.1007/BF02165690
10. Nagy S, Kuzmann E, Weiszburg T, Gyökeres-Tóth M, Riedel M (2000) Oxide transformation during preparation of black pottery in Hungary. J Radioanal Nucl Chem 246:91–96. https://doi.org/10.1023/A:1006733131174
11. Hanesch M (2009) Raman spectroscopy of iron oxides and oxy(hydroxides) at lower laser power and possible application in environmental magnetic studies. Geophys J Int 177:941–948. https://doi.org/10.1111/j.1365-246X.2009.04122.x
12. Cornell RM, Schwertmann U (2003) The Iron Oxides: Structure, Properties, Reactions, Occurrences and Uses. Wiley-VCH, Weinheim
13. Byrne J, Kappler A (2019) Mössbauer spectroscopy, analytical geomicrobiology: a handbook of instrumental techniques. Cambridge University Press, Cambridge
14. Cudennec Y, Lecerf A (2005) Topotactic transformations of goethite and lepidocrocite into hematite and maghemite. Solid State Sci 7:520–529. https://doi.org/10.1016/j.solidstatesciences.2005.02.002
15. Fang J, Kumbar A, Zhou WL, Stokes KL (2003) Nanoneedles of maghemite iron oxide prepared from a wet chemical route. Mater Res Bull 38:461–467. https://doi.org/10.1016/S0025-5408(02)01066-8
16. Gorski CA, Scherer MM (2010) Determination of nanoparticulate magnetite stoichiometry by Mössbauer spectroscopy, acidic dissolution, and powder X-ray diffraction: A critical review. Am Mineral 95:1017–1026. https://doi.org/10.2138/am.2010.3435
17. Jeon AY, No HG, Kim US, Cho WS, Kim KJ, Kim JY, Kim CM, Kim CS, Kang KI (2012) Systematic study on colorative mechanism of ancient goryeo celadon glaze by mossbauer spectroscopy and chromaticity analysis J Korean Ceram Soc 49:66–71. https://doi.org/10.4191/kcers.2012.49.1.066 **(in Korean with English abstract)**

Publisher's Note Springer Nature remains neutral with regard to jurisdictional claims in published maps and institutional affiliations.